Epigenetics Communications

RESEARCH

Open Access

Changes in histone lysine acetylation, but not DNA methylation during facultative hibernation in Syrian hamster liver

Marloes M. Oosterhof[1,2†], Louis Coussement[3†], Alienke van Pijkeren[4,5], Marcel Kwiatkowski[5,6], Martijn R. H. Zwinderman[7], Frank J. Dekker[7], Tim de Meyer[3], Vera A. Reitsema[1], Rainer Bischoff[4], Victor Guryev[8], Hjalmar R. Bouma[1,9], Rob H. Henning[1] and Marianne G. Rots[2*]

Abstract

Background Hibernation (torpor) is a strategy to survive extreme environmental conditions, associated with a significant decrease in metabolism and body temperature. The inducibility by the environment of torpor for facultative hibernators designates epigenetic mechanisms as likely candidates for regulation. Therefore, we set out to unravel epigenetics in the liver of a facultative hibernator, Syrian hamster (*Mesocricetus auratus*), sampled at different phases during hibernation, by assessing the expression of epigenetic writer and eraser enzymes, histone acetylation dynamics, and DNA methylation levels.

Results Expression of epigenetic writers/erasers confirmed previously reported results obtained in obligatory hibernators, but might point to a mechanism specific for facultative hibernators, e.g., differential expression of histone acetyltransferases (HATs; *KAT6A*, *KAT6B*, *KAT7*, and *KAT13D/CLOCK*). These findings were in accordance with observed changes in histone H3 and H4 acetylation changes. Overall histone deacetylase (HDAC) activity was highest in torpor. No differences were detected in DNA methylation throughout all phases.

Conclusion Our study thus points to histone acetylation as an important player in facultative hamster hibernation, which may underlie the orchestration of gene expression changes throughout hibernation.

Keywords HDAC, HAT, RNA sequencing, Epigenetics, Histone acetylation, WGBS

†Marloes M. Oosterhof and Louis Coussement contributed equally to this study.

*Correspondence:
Marianne G. Rots
m.g.rots@umcg.nl
[1] Department of Clinical Pharmacy and Pharmacology, University of Groningen, University Medical Center Groningen, Groningen, The Netherlands
[2] Department of Pathology and Medical Biology, University of Groningen, University Medical Center Groningen, Groningen, The Netherlands
[3] Department of Data Analysis and Mathematical Modelling, Faculty of Bioscience Engineering, Ghent University, Ghent, Belgium
[4] Department of Analytical Biochemistry, Groningen Research Institute of Pharmacy, University of Groningen, Groningen, The Netherlands
[5] Institute of Biochemistry and Center for Molecular Biosciences Innsbruck, University of Innsbruck, Innsbruck, Austria
[6] Department of Pharmacokinetics, Toxicology and Targeting, Groningen Research Institute of Pharmacy, University of Groningen, Groningen, The Netherlands
[7] Department of Chemical and Pharmaceutical Biology, Groningen Research Institute of Pharmacy, University of Groningen, Groningen, The Netherlands
[8] European Research Institute for the Biology of Ageing, Groningen, The Netherlands
[9] Department of Internal Medicine, University of Groningen, University Medical Center Groningen, Groningen, The Netherlands

Background

Hibernation is an adaptive strategy to cope with low energy supplies and/or challenging environmental conditions. Consistent with a need to reduce energy consumption during torpor, several studies have demonstrated reduced gene transcription and protein synthesis in hibernators [1–3]. There are two types of hibernators, obligatory and facultative [4]. The former shows seasonal hibernation irrespective of environmental conditions but driven by a circannual rhythm [4, 5]. In contrast, facultative hibernators deploy torpor in response to particular environmental cues, including shortening of days, scarcity of food, and low ambient temperatures [6].

Dietary glucose is unavailable during the fasting period of hibernators; hibernators need a switch to fatty acid oxidation to maintain cellular energy supply [7, 8]. Additionally, it is suggested that facultative hibernators arouse regularly to maintain blood glucose levels through glycogenolysis or gluconeogenesis from available metabolites of the TCA cycle [9]. These processes are mainly regulated by the liver, which has a central role in maintaining the metabolic homeostasis of the whole animal. Given its key roles in hibernation including gluconeogenesis, ketogenesis, and protein synthesis, we here, as in many other hibernation studies, focus on the liver [10–12].

Since metabolism and epigenetic regulation of gene expression clearly interlink [13], we aim to address the role of epigenetic regulation in hibernation either as a cause or a consequence of the metabolic changes in facultative hibernators. We focus on histone acetylation, which is typically associated with an "open" chromatin structure allowing transcription factors to bind the DNA. In general, histone lysine (K) acetylation on histone H3 and H4 (H3KAc, H4KAc) is a well-studied histone modification often accompanied and/or induced by a change of metabolic processes [13]. Next to changes in histone acetylation throughout hibernation phases, also changes in protein levels of histone acetyltransferase (HAT) and histone deacetylase (HDAC) were reported [14, 15]. Moreover, HAT and HDAC activity increased in specific tissues of ground squirrels during torpor [14, 16]. Finally, previous reports in ground squirrels and chipmunks showed differential regulation of acetylation of histones in different tissues, including the liver [14, 17–19].

In fat, and recently liver tissue of ground squirrels, it was found that transcription is reduced during torpor [14, 20]. DNA methylation is generally associated with gene silencing making it a plausible mechanism of gene silencing in torpor. Few studies have been performed on DNA methylation in hibernators [21], indicating for example a decrease in genome-wide DNA methylation for arousing obligatory hibernators (ground squirrel) compared to euthermic controls housed at 4 °C (despite increased expression of *DNMT1/3B* and *MBD2*) [22, 23]. Also, *MBD3* and *MECP2* mRNA expression was increased in arousal compared to euthermic animals. On the other hand, for the facultative hibernator, the chipmunk (*Tamias striatus*), stable DNA hypermethylation was found for promoter regions of *HP-20*, *HP-25*, and *HP-27*, despite changes in histone acetylation, during torpor compared to summer euthermic [18, 19].

Given previous evidence of epigenetic regulation in obligatory hibernators [3], we interrogated epigenetics in the liver of the facultative hibernator, Syrian hamster (*Mesocricetus Auratus*). We used untargeted approaches to study epigenetics (RNA-seq, Luminometric Methylation Assay (LUMA), and Whole Genome Bisulfite Sequencing (WGBS)) and assessed histone acetylation levels (Western Blot and LC-MS/MS) and measured the activity of HATs and HDACs in livers of Syrian hamsters during different phases of hibernation. Unraveling the regulation of epigenetic modifications in the facultative hibernating Syrian hamster offers insight into the orchestration of gene expression changes in preparation of and during hibernation. Furthermore, their "hibernation-on-command" triggering hypometabolic and cytoprotective mechanisms might provide an interesting model to address fundamental questions in human pathophysiology, e.g., prevention of ischemic damage during organ transplants. Recently, epigenetic aging has been described to be essentially stalled during hibernation periods [24], further highlighting the relevance of understanding the epigenetic processes driving hibernation.

Methods

Ethical approval

Experiments were approved by the Institutional Animal Ethical Committee of the University Medical Center Groningen. Animal procedures were carried out in accordance with the European Directive on the Protection of Animals used for Scientific Purposes and Dutch legislation. Experiments were performed on Syrian hamsters from Envigo (Indianapolis, USA) with food and water ad libitum. Euthanasia was performed by exsanguination under isoflurane anesthesia.

Animals

Twenty Syrian hamsters (12 weeks of age, 10 males and 10 females) were housed at an ambient temperature of 21 °C, a light:dark cycle (L:D cycle) of 14:10 h and food ad libitum (Additional file 1). Hibernation was induced by shortening the L:D cycle to 8:16 h for 10 weeks followed by housing at an ambient temperature of 5 °C, at continuous dim light (<5 Lux) [25]. Food was removed after the animals entered torpor. The hibernation patterns of

animals were determined by continuous assessment of movement via infrared detectors connected to a computer. Syrian hamsters with >24 h of inactivity were considered torpid [26]. Animals were euthanized by exsanguination under isoflurane anesthesia during summer, torpor, or interbout arousal, the final duration of the last uninterrupted torpor bout of hibernating animals lasting >80 h for all animals. Animals were euthanized in torpor late (TL, > 72 h after entrance into torpor), arousal early (AE, 1.5 h after cessation of torpor), and arousal late (AL, 6–8 h after cessation of torpor). Summer Euthermic (SE) animals were housed at 21 °C and a light:dark cycle (L:D cycle) of 14:10 h. The animal's activity pattern accurately identified hibernating hamsters as being in torpor or arousal, as evidenced by mouth temperature (Tm) at euthanization (Additional file 1). Arousals were induced by the handling of the animals. The liver was obtained and snap-frozen in liquid nitrogen and stored at −80 °C.

Protein extraction and immunoblotting

Liver tissue ($n = 5$ per group) was homogenized in an ice-cold homogenizing buffer, and protein was extracted using RIPA buffer. Protein concentrations were determined using Biorad DC assay. Equal amounts of proteins were loaded onto SDS-polyacrylamide gels and separated using an electrophoresis cell. Membranes were blocked using skim milk (5%, 30 min) in tris-buffered saline with Tween 20 (TBST) and probed with specific primary antibodies 1:1000 in 3% BSA o/n (Table 1). Membranes were incubated with secondary anti-rabbit or anti-mouse IgG HRP-linked antibody (1:2000 in 3% BSA) for 1 h at room temperature and developed using enhanced chemiluminescence. Protein intensities were corrected for background and a loading control was used to normalize blots using Image Lab (Biorad).

Luminometric Methylation Assay (LUMA)

LUMA was performed using genomic DNA (gDNA) isolated with Nucleospin Tissue (Machery qNagel). gDNA was digested with EcoRI and HapII (5mC sensitive) or MspI (5mC insensitive) in Q24 pyrosequencer for 4 h at 37 °C, followed by 20 min at 80 °C. Subsequently, the nucleotides were added and run in the Pyromark Q24 system. Readout was analyzed using Pyromark design.

Tissue lysis and histone protein extraction

Liver tissue ($n = 4$ per group) was homogenized in 1 mL of ice-cold lysis buffer containing PBS and 0.5% Triton X-100 (v/v) with a pDEGrotease inhibitor (1 mM PMSF) and histone deacetylase inhibitors (1 mM sodium butyrate, 10 µM SAHA and 10 mM nicotinamide) using a sonicator (3 tunes, 10 s, 50%, on ice) and samples were centrifuged for 10 min at 10,000×*g* at 4 °C. After discarding the supernatant, pellets were resuspended in 0.5-mL ice-cold buffer containing 13 mM EDTA in 10 mM Tris-base, pH 7.4. After centrifugation (10 min at 10,000×*g*, 4 °C) and discarding of the supernatant, pellets were resuspended in 200-µL ice-cold HPLC grade water (HPLC-H_2O). Sulfuric acid (H_2SO_4) was added to the samples to a final concentration of 0.4 M. Samples were incubated on ice for 1 h with gentle agitation. After centrifugation (10 min at 10,000×*g* 4 °C), the supernatant containing the histone proteins was added to 1.5 mL acetone and left at −20 °C overnight to precipitate the proteins. After centrifugation, acetone was removed and the pellet was dried at room temperature. The pellet was subsequently reconstituted in 50 µL HPLC-H_2O. Protein concentration was determined using the microplate BCA protein assay kit (Thermo Fisher, Waltham, USA) following the manufacturer's instructions using a BSA standard (2 mg/mL). The absorbance was measured at 580 nm using a microplate reader.

Chemical acetylation and in-solution digestion

Extracted histone proteins were diluted in HPLC-H_2O to 12 µg/µl. The protein disulfide bridges were reduced with 1 µL of 100 mM DTT (10 min, 57 °C). After reduction, alkylation was performed with 1 µL 300 mM iodoacetamide (30 min, in the dark at room temperature). Subsequently, 35 µL of 180 mM sodium borate buffer was added and pH was adjusted to pH 8.5. Next, 1 µL 2% deuterated acetic anhydride in DMSO was added and incubated for 10 min on a thermomixer (1000 rpm) at RT. The acetylation reaction was performed in triplicate. To revert possible O-acetylation, hydroxylamine solution was added to an end concentration of 0.25 µg/µL and the samples were incubated on a thermomixer (450 rpm) at RT for 120 min. Overnight digestion was performed with 1 µL trypsin solution (0.2 µg/µL sequencing

Table 1 Antibodies used for immunoblots

Antibody	Article reference
Acetyl-Histone H3 (Lys27) (D5E4) XP® Rabbit monoclonal antibody	Cell signaling, Cat# 8173s
Histone H3 (96C10) Mouse monoclonal antibody	Cell signaling, Cat# 3638
Anti-Histone H3 (acetyl K9) polyclonal antibody	Abcam, Cat# Ab4441
Anti-Histone H3 (acetyl K9 + K14 + K18 + K23 + K27) polyclonal antibody	Abcam, Cat# Ab47915

grade modified trypsin, dissolved in trypsin resuspension buffer) at 37 °C. The samples were acidified by adding formic acid.

Histone acetylation quantification using LC-MS/MS

LC-MS/MS using a quadrupole orbitrap mass spectrometer (Orbitrap QExactive Plus, Thermo Scientific, Bremen, Germany) coupled to a nano-ultra pressure liquid chromatography system (Dionex UltiMate 3000 RSLCnano pro flow, Thermo Scientific, Bremen, Germany) coupled via electrospray-ionization (ESI) analysis were performed as described earlier [27].

LC-MS/MS data analysis was performed with Freestyle 1.6 (Version 1.6.75.20, Thermo Scientific, Bremen, Germany). Extracted ion chromatograms (EICs) of the acetylated histone isotopologue species were generated using the following parameters: detector type: MS, trace type: mass range, ranges: theoretical m/z of the corresponding acetylated histone isotopologue species, mass tolerance: 8 ppm, peak detection algorithm: Genesis, percent of highest peak: 10, minimum peak height S/N: 5, S/N threshold: 3, tailing factor: 5.

HDAC activity

Fifty-microgram protein from liver tissue was isolated in × Passive lysis buffer (Promega, Madison, WI, USA) according to the manufacturer's protocol. Histone deacetylase (HDAC) activity was measured in duplicate (n = 3 per group) using HDAC activity colorimetric assay kit (Cat. No. K331-100) from BioVision Inc. (Milpitas, CA, USA) according to the manufacturer's instructions. Incubation was done simultaneously for 1 h at 8 °C, 21 °C, and 37 °C for all samples in different plates before stopping the reaction using Lysine developer. The colorimetric readings were measured at 400 nm in a spectrophotometer.

HAT activity

Twenty-microgram protein from liver tissue was isolated in 1× Passive lysis buffer (Promega). HAT activity was measured in duplicate (n = 3 per group) using EpiQuik™ HAT Activity/Inhibition Assay Kit (Epigentek Cat. No. P-4003, Farmingdale, NY, USA) according to the manufacturer's instructions. The absorbance was measured at 450 nm in a microplate reader.

RNA sequencing data and Whole Genome Bisulfite Sequencing (WGBS) data

Expression measurements and DNA methylation measurements were obtained from previously published work by the groups collaborating on this project [8]. Extraction of the respective material, (pre)processing and normalization of raw data, and statistical analyses were performed as described there. The raw data for these analyses can be found in the Gene Expression Omnibus (GEO) under accessions GSE199814 and GSE199815 for RNA sequencing and WGBS data respectively. Of importance is that material for RNA sequencing and WGBS was retrieved from the same three samples (out of five) within the respective SE, AE, and TL groups from which protein extraction was performed.

Statistical analysis

Results are presented as mean ± standard error of the mean (s.e.m.), with dots in figures showing the values of individual animals. The Kruskal-Wallis test with a Dunn's correction for multiple group comparisons was performed. P-values < 0.05 were considered statistically significant. Graphpad Prism version 8.4.2 was used for all statistical evaluations.

Results

In order to assess the role of epigenetics in hibernation, we analyzed mRNA expression (RNA-seq), DNA methylation (LUMA and WGBS), and histone acetylation with accompanying HDAC and HAT activity data. Measurements for these different modalities contributing to hibernation states in the facultative hibernator, Syrian hamsters, were performed on the same (subset) of animals to facilitate integration and interpretability (see Additional file 1 for a comprehensive overview of which samples were included for different modalities). We start by examination of expression levels for epigenetic writers and erasers, followed by an assessment of acetylation levels and finally measurement of DNA methylation throughout the different phases of hibernation.

Differential expression of epigenetic writers and erasers in torpor or arousal

Differential expression (DE) results were analyzed using our previously published RNA-seq data set [8] for 94 pre-selected enzymes (based on literature and in-house expertise) including all known HATs, HDACs, histone methyltransferases (KMTs), histone demethylases (KDMs), DNA methyltransferases (DNMTs) and ten-eleven translocation methylcytosine dioxygenases (TETs). In short, this experiment compared gene expression in Syrian hamster livers sampled at different phases of hibernation: summer euthermic (SE), torpor late (TL: >72 h after the entrance to torpor), and arousal early (AE: 1.5 h after the start of arousal) [8]. Expression levels for 11 genes in our selection (*HDAC9*, *DNMT3B*, *TET1*, and 8 KMTs) could not be determined due to low coverage or missing assembly (Additional file 2 for full DE results). Of the remaining 83 genes (37 histone-modifying enzymes and 46 DNA

methylation-associated proteins), 11 genes were found to be differentially expressed in at least one comparison between the three hibernation phases (false discovery rate, FDR < 0.05, Fig. 1). More specifically, seven genes encode histone acetyltransferases and deacetylases (Fig. 1A), three encode histone methylation-modifying

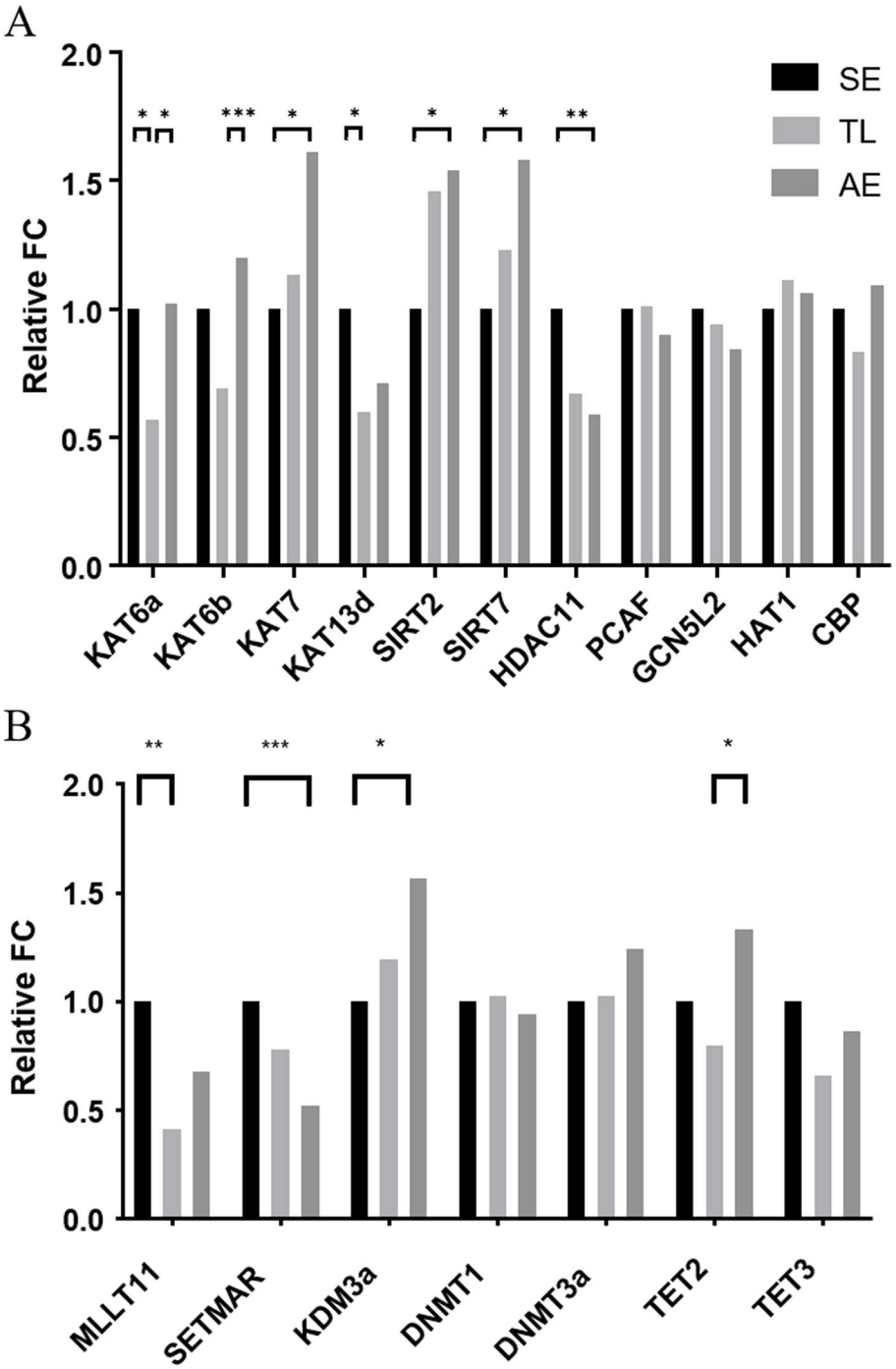

Fig. 1 Relative fold changes from differential expression analysis for 18 genes encoding epigenetic enzymes, including the 11 differentially expressed genes (FDR < 0.05). Bars indicate relative fold change compared to expression for SE animals (hence SE bars are all equal to 1). The selection of genes included in this plot is based on detectable presence in RNA sequencing data. **A** Genes modifying histone acetylation. **B** Genes modifying histone and DNA methylation. RNA was subjected to sequencing for livers derived from summer euthermia (SE), torpor late (TL), and arousal early (AE) hamsters ($n = 3$ per group). Statistical analysis was performed using Kruskal-Wallis *$P < 0.05$; **$P < 0.01$

enzymes, and the *TET2* gene encodes a DNA demethylating enzyme (Fig. 1B). Effect sizes (fold change, FC) and significance levels for these eleven differentially expressed genes are represented in Fig. 1.

Of the 21 known and detected HATs, four were differentially expressed of which expression for 3 HATs was decreased during torpor (Fig. 1A). *KAT6A* was downregulated in TL compared to both SE and AE (1.74-fold and 1.78-fold, respectively; FDR < 0.05). For *KAT6B*, the downregulation reached statistical significance for TL compared to AE animals (1.72-fold; FDR < 0.001). *KAT13D* (also known as *CLOCK*, a circadian gene found to mediate HAT activity) showed a decreased expression in TL compared to SE (1.67-fold; FDR < 0.05). In contrast, *KAT7* showed an opposite pattern: unchanged in TL but upregulated in AE compared to SE (1.61-fold; FDR < 0.05). Expression for *SIRT2* and *SIRT7*, NAD^+ utilizing Class III HDACs, was resp. 1.54- and 1.58-fold increased during arousal compared to summer euthermic (SE) animals (both FDR < 0.05). One other HDAC showed differential expression (*HDAC11*, a class IV HDAC), but here an opposite pattern was observed with AE animals showing a 1.68-fold reduction in expression compared to SE animals (FDR < 0.01). While the expression of these three identified HDACs (*SIRT2*, *SIRT7*, and *HDAC11*) differed between SE and AE, neither two phases differed significantly from TL. Remarkably, none of the previously reported differentially expressed histone-modifying enzymes in 13-lined ground squirrel, *PCAF*, *GCN5L2*, *HAT1*, and *CBP* [15], showed differences in expression in hibernating hamster compared to SE (Fig. 1A, Additional file 2).

Next, we explored methylation-modifying enzymes. A total of 46 enzymes were identified as expressed in the liver, including KDMs, DNMTs, and TETs (Fig. 1B). For KMTs, only two genes were differentially expressed. *MLLT11* showed a 2.43-fold reduction in expression in TL compared to SE (FDR < 0.001), whereas *SETMAR* showed a 1.91-fold reduction in expression in AE compared to SE (FDR < 0.01). For KDMs, only *KDM3A* was differentially expressed, showing a similar pattern to *SIRT2*, *SIRT7*, and *KAT7*, as it was upregulated in AE compared to SE (1.56-fold; FDR < 0.05). Lastly, for DNMTs and TETs, only *TET2* showed differential expression with a 1.67-fold increase in expression in AE compared to TL (FDR < 0.05). No other DNA methylation-modifying enzymes, including the previously reported hibernation-associated *DNMT1* [22] showed differential gene expression between any of the groups (Fig 1B). Altogether, of the 83 detected epigenetic enzymes, four HATs, three HDACs, two KMTs, one KDM, and one TET were found to be differentially expressed (Fig. 1A, B).

Histone H3 acetylation is differentially regulated across the hibernation cycle

Given the differential expression of some HATs and HDACs, we next assessed histone H3 acetylation (H3ac) using Western Blot (WB). Because nine of the eleven DEGs were differentially expressed in AE, five samples were obtained from hamsters in arousal late (AL: >8h after the start of arousal) and included to expand the assessment of histone modifications in the arousal phase.

First, H3 protein levels were measured to ensure stable levels throughout the hibernation cycle (Fig. 2A; representative sample for WB images in Additional file 3). Overall H3 acetylation status, normalized to H3 levels, was lower in TL livers compared to AL ($P < 0.05$; Fig. 2B). Next, we assessed the acetylation status of the two most commonly studied lysine sites (H3K9 and H3K27; Fig. 2C, D). H3K9ac decreased during the hibernation phases, reaching statistical significance in AL compared to SE animals (Fig. 2C). H3K27ac followed the same pattern observed for overall H3ac, with the lowest levels detected in TL compared to AL (Fig. 2D). Differences observed for TL versus AL livers were independent of normalization for H3 protein levels per sample. Note that this reduction of acetylation in torpor coincides with significant downregulation of HATs (see previous section) and the increase in acetylation in arousal coincides with the upregulation of KAT7 during arousal.

Differential levels of histone H3 and H4 acetylation across hibernation phases

The differences in H3ac were validated and expanded for other lysines using quantitative LC-MS/MS analysis on the same ($n = 4$) liver samples from SE, TL, and AL hamsters, as these groups showed the most prominent changes. Given that the hibernation-associated DEGs encode HATs and HDACs which also target histone H4 lysine sites in addition to H3 lysine sites (Fig. 3), the analysis was expanded to include four H4 lysine residues (H4K5, H4K8, H4K12, and H4K16; Fig. 4). The acetylation stoichiometries of H3K4, H3K9, H3K14, H3K36, and H4K20 could not be investigated with the assay used because these peptides were not sufficiently retained by the trapping and separation column.

The analyzed H3(18–26) peptide K18QLATK23AAR contained two acetylation sites, K18 and K23, and can be either unacetylated, acetylated at one site (monoacetylated), or acetylated at both sites (diacetylated). As shown in Fig. 3A, most of the H3(18–26) peptide species were unacetylated (71.1%), followed by the monoacetylated (22.5%) and the diacetylated peptides (6.4%). In line with the WB data, the H3(18–26) peptide showed a significant decrease in acetylation in TL as shown for both the mono- and diacetylated peptides (Fig. 3A,

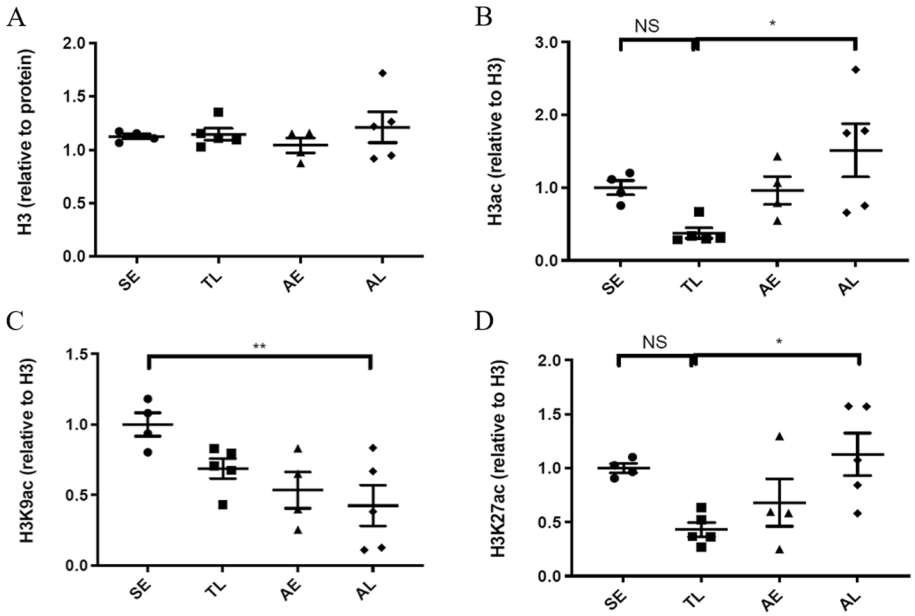

Fig. 2 Histone H3 protein acetylation in the liver of hibernating hamster. **A** Overall histone H3 protein levels relative to total protein amount. **B** Histone H3 pan-acetyl lysine levels. **C** Histone H3 acetylation at lysine 9. **D** Histone H3 acetylation at lysine 27. **B**–**D** Data are normalized to total histone H3 protein levels (**A**). Data are relative to the mean of SE and presented as mean ± s.e.m. Statistical analysis by Kruskal-Wallis with Dunn's correction **P* < 0.05; ***P* < 0.01

B). Further analyses indicated that both H3K18ac and H3K23ac decreased in acetylation during torpor (~4.6% for H3K18ac; ~14.0% for H3K23ac, Fig. 3C). In contrast, no significant changes in acetylation were observed for H3K27 or H3K79 in TL liver (Fig. 3C). Subsequently, assessing acetylation of specific lysine residues, an increase in acetylation was found for H3K23 (~13.1%) and H3K27 (~6.9%) in AL vs TL ($P < 0.05$, Fig. 3C, D), signifying that the pattern found for H3K27ac by WB (Fig. 2D) was confirmed by LC-MS/MS measurements. The overall H3ac pattern obtained for H3K9, K14, K18, K23, and K27 by WB (Fig. 2B) thus corresponds to the results of the H3K18ac and H3K27ac lysines measured by LC-MS/MS, identifying K9ac as an interesting H3 lysine with sustained decreased acetylation in AL vs SE (Fig. 2C).

The analyzed H4 peptide, H4(4–17) (GK5GGK8GLGK12GGAK16R), can be either unacetylated or acetylated at one to four lysine residues. Most of the peptide is in its unacetylated state (average of 54.7%) followed by the monoacetylated peptide (37.3%) and diacetylated peptide (4.8%). A very small subset of the peptide is acetylated at three or all four lysine sites (<3%). In contrast to H3ac, for which the reduced acetylation levels in TL were generally restored in AL, the level of acetylated H4(4–17) peptide remained decreased in AL compared to SE (Fig. 4A, B). In all hibernation phases, approximately 45.3% of the H4 peptide was acetylated, of which the majority was only acetylated once. For the monoacetylated peptide, the distribution of acetylation over the four different lysine residues was measured (Fig. 4A). Markedly, most of the monoacetylated peptides were acetylated at H4K16, with a significant decrease in H4K16ac in AL compared to both the SE and TL animals (Fig. 4A, C). Moreover, H4K12ac monoacetylation showed a significant decrease in AL versus TL. However, as indicated in Fig. 4A and C, the contribution of H4K12ac to the total amount of monoacetylation is small.

HDAC activity is increased in late torpor

Given the changes in the acetylation levels of histone lysines, we next explored the enzymatic activity of the acetylation writers and erasers. HAT activity remained similar throughout all four hibernation phases ($n = 3$; Fig. 5A). Conversely, HDAC activity measured at 37 °C in the same tissue samples was upregulated in TL compared to AE (Fig. 5B). Because of differences in HDAC activity between TL and AE at 37 °C, liver HDAC activity was also measured at the temperature corresponding to the animals' body temperature at the time of procurement, but differences between phases were maintained irrespective of assay temperatures (Additional file 4).

A

H3 (18-26)	SE (n = 4) Mean % ± s.e.m.	TL (n = 4) Mean % ± s.e.m.	AL (n = 4) Mean % ± s.e.m.
Unacetylated	65.5 ± 0.5	80.1 ± 0.8	67.7 ± 2.3
1x acetylated	26.0 ± 0.7	15.5 ± 0.5	26.1 ± 1.6
2x acetylated	8.5 ± 1.1	4.4 ± 0.5	6.2 ± 0.9

B

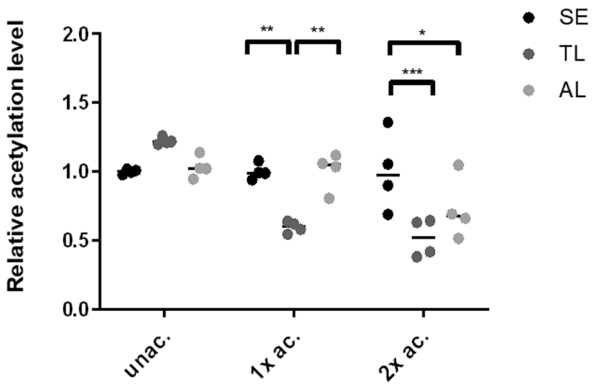

C

	SE (n = 4) Mean % ± s.e.m.	TL (n = 4) Mean % ± s.e.m.	AL (n = 4) Mean % ± s.e.m.
H3K18ac	12.4 ± 5.0	7.8 ± 2.5	10.1 ± 5.4
H3K23ac	30.6 ± 3.5	16.6 ± 1.6	29.7 ± 2.3
H3K27ac	18.0 ± 4.8	15.1 ± 4.2	22.0 ± 6.9
H3K79ac	0.2 ± 0.9	0.2 ± 0.6	0.1 ± 1.0

D

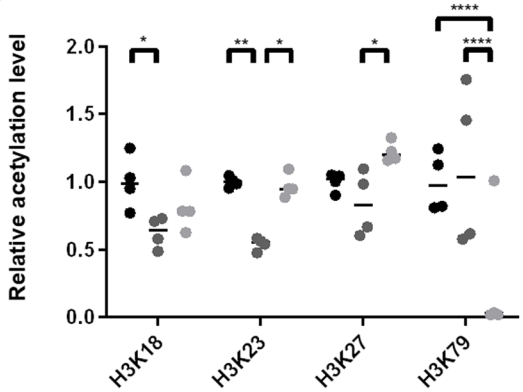

Fig. 3 Absolute and relative H3 acetylation levels in the liver of the Syrian hamster measured by LC-MS/MS. **A** Overall acetylation of the H3(18–26) peptide (KQLATKAAR). Unacetylated, single, or double acetylated H3(18–26) levels are expressed as a percentage of the total. **B** Relative levels of the unacetylated, single, or double acetylated H3(18–26) peptide. **C** Relative site-specific acetylation levels for H3K18, H3K23, H3K27, and H3K79. Levels are relative to the mean of SE. **D** Lysine-specific acetylation of H3 lysines. H3K18 and H3K23 are determined using one H3 peptide (K_{18}QLATK_{23}AAR); H3K27 is the only acetylated site within the assessed peptide K_{27}SAPATGGV$K_{36}K_{37}$PHR; as is H3K79 in the peptide EIAQDFK_{79}TDLR. Measurements were performed for summer euthermic (SE), torpor late (TL), and arousal late (AL) animals. All relative levels are calculated compared to the mean of SE. Statistical analysis was performed using Kruskal-Wallis with Dunn's correction **P* <0.05, ***P* < 0.01, *****P* < 0.0001

Increase in HDAC6 activity is associated with increased histone deacetylation, but not with tubulin deacetylation

To further identify HDACs with increased activity in TL, activity assays with HDAC inhibitors were performed using reported IC50s [28, 29]. Inhibitors showed similar activity on liver samples from SE, TL, AE, and AL animals (Additional file 5) and representative findings are shown for SE animals (Fig. 6A). Treatment with the pan HDAC inhibitor, Vorinostat, inhibited HDAC activity by 99%. Class I HDAC inhibitor Entinostat (MS-275) reduced the overall activity by 22.0 ± 0.08% ($P < 0.01$). Tubastatin A, an inhibitor of HDAC6, inhibited the overall activity by 71.0 ± 0.03% ($P < 0.001$). As HDAC6 is largely known for deacetylating α-tubulin [30], levels of acetylated α-tubulin were measured in the liver using Western blot (Fig. 6B), to further evaluate increased HDAC6 activity. Remarkably, the percentage of acetylated α-tubulin significantly increased in TL versus SE and AL.

LUMA and WGBS results showed no global changes in DNA methylation

To investigate overall DNA methylation changes during hibernation, DNA methylation was assessed using LUMA on the same liver samples as used for RNA-seq with the result that no changes in overall DNA methylation were detected (Additional file 6). To explore DNA methylation status in depth, previously published WGBS was reanalyzed. No significant differences were found for overall cytosine methylation of CpG and non-CpG sites between different hibernation phases (resp. Additional file 7, panels A and B). Furthermore, promoter methylation of DEGs showed no clear differences in average methylation between hibernation phases ($P = 0.74$, Additional file 7, panel C). However, upon a detailed assessment of overall CpG methylation for genic regions of DEGs, there are minor indications of lower methylation for euthermic animals compared to TL animals (2.9%, $P = 0.07$) and arousal animals (3.0%, $P < 0.12$) (Additional

A

H4 (4-17)		SE (n = 4) Mean % ± s.e.m.	TL (n = 4) Mean % ± s.e.m..	AL (n = 4) Mean % ± s.e.m.
unacetylated		48.8 ± 1.6	53.3 ± 0.6	62.0 ± 1.8
1x acetylated		39.6 ± 0.9	40.7 ± 0.8	31.5 ± 0.6
	H4K5	*1.4 ± 0.1*	*1.0 ± 0.1*	*1.1 ± 0.1*
	H4K8	*2.5 ± 0.1*	*2.4 ± 0.2*	*2.4 ± 0.3*
	H4K12	*1.2 ± 0.1*	*2.2 ± 0.1*	*0.7 ± 0.1*
	H4K16	*34.5 ± 0.7*	*35.3 ± 0.7*	*27.3 ± 0.7*
2x acetylated		6.5 ± 0.5	3.7 ± 0.3	4.3 ± 0.6
3x acetylated		2.3 ± 0.3	1.1 ± 0.1	1.2 ± 0.5
4x acetylated		2.9 ± 0.4	1.2 ± 0.3	0.9 ± 0.4

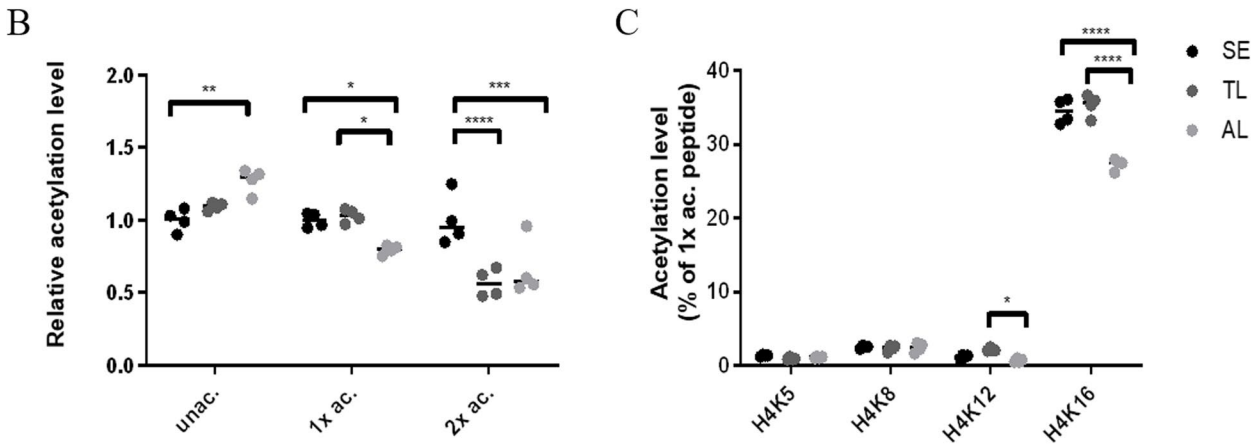

Fig. 4 Absolute and relative acetylation levels of the H4(4–17) peptide (GKGGKGLGKGGAKR) in the liver of the Syrian hamster measured by LC-MS/MS. **A** Acetylation levels of the H4(4–17) peptide for unacetylated or acetylated at one, two, three, or four (all) lysine residues. The distribution (%) of the specific lysine residue (H4K5, H4K8, H4K12, and H4K16) for the singly acetylated H4(4–17) peptide is specified. **B** Relative levels of the unacetylated, single, or double acetylated H4(4–17) peptide. Data are represented as mean (relative to the mean of SE). **C** Distribution of the singly acetylated H4(4–17) peptide at the four lysine residues H4K5, H4K8, H4K12, and H4K16. Acetylation levels were measured for summer euthermia (SE), torpor late (TL), and arousal early (AE) hamsters ($n = 4$ per group). Acetylation levels of the single lysine residues are shown as percentage of the total H4(4–17) peptide. All relative levels are calculated compared to the mean of SE. Statistical analysis by Kruskal-Wallis with Dunn's correction *$P < 0.05$, **$P < 0.01$, ***$P < 0.001$, ****$P < 0.00001$

file 7, panel D). The limited differences in RNA expression for the writers and maintenance enzymes for DNA methylation (e.g., DNMT1 and DNMT3a, Fig. 1B) are in accordance with the lack of global changes in DNA methylation during hibernation.

Discussion

Hibernation is a dynamic process accompanied by essential physiological changes, which are thought to be under transcriptional control [3, 16]. In this study, we assessed the expression levels of 94 epigenetic writers and erasers. Expression of 83 genes encoding epigenetic proteins sufficed to assess differential mRNA expression, which was observed for 11 of the genes. Due to the exploratory nature of this study, we did not confirm the changes in gene expression using qRT-PCR. It is likely that the changes reported in our bulk analyses largely represent those in hepatocytes, being the most abundant cell type (80+ %). Detailed changes in less abundant cell types, such as stellate and Kupfer cells, await further analyses using sorted or single-cell sequencing techniques in follow-up studies. Given its role as a dynamic modification, highly involved in changes in metabolism [13], we focused on histone acetylation as transcriptional regulator. We found an increased HDAC activity in torpor, which was not observed for HATs. This increased HDAC activity was associated with a decrease in H3K18, H3K27, and H3K23 acetylation during torpor compared to aroused animals. Furthermore, decreased levels of H4K12 and H4K16 acetylation were observed in arousal.

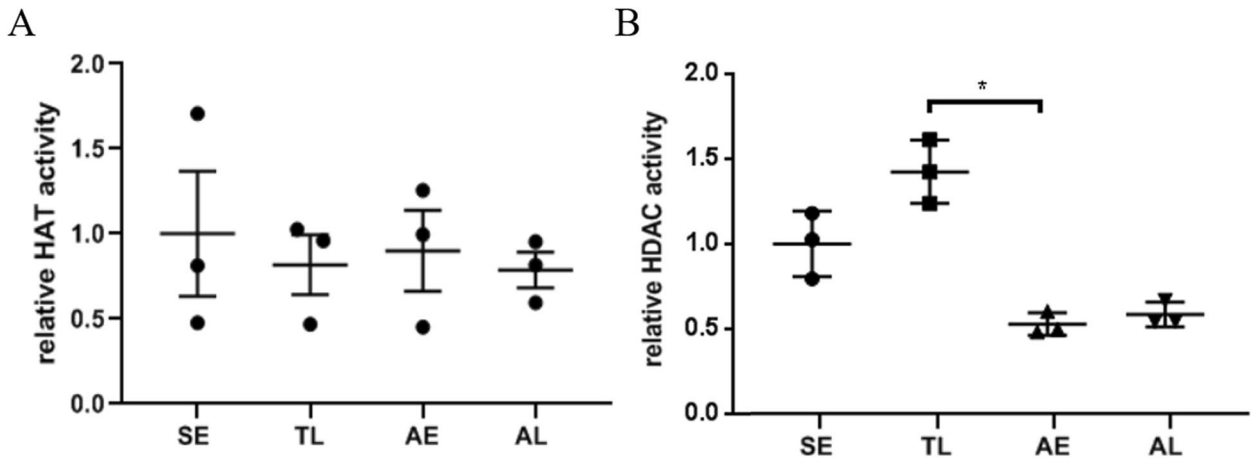

Fig. 5 HAT and HDAC activity during the torpor-arousal cycle. **A** HAT activity. **B** HDAC activity. Activity was measured for summer euthermic (SE), torpor late (TL), and arousal late (AL) measured at 37 °C. Data represented as mean ± S.E.M and are relative to the mean of SE. Statistical analysis by Kruskal-Wallis with Dunn's correction **P* < 0.05

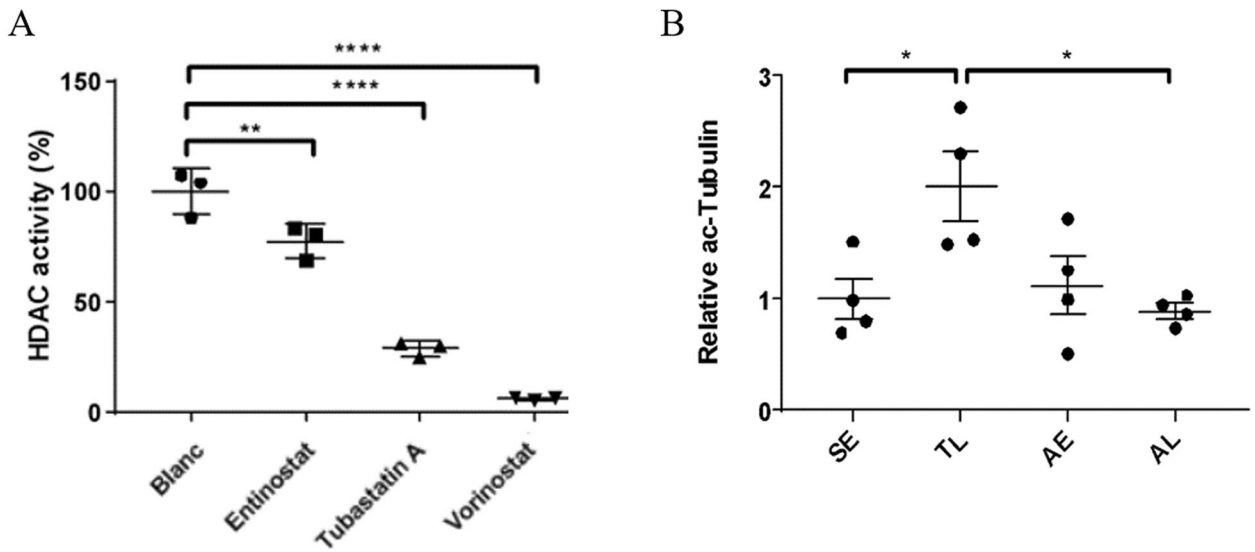

Fig. 6 HDAC activity and ac-tubulin in Syrian hamster liver. **A** HDAC activity in SE animals (*n* = 3) using inhibitors: Entinostat to inhibit class I HDACs, Tubastatin A to inhibit HDAC6, and Vorinostat to inhibit all HDACs, except Sirtuins. **B** Levels of acetyl-tubulin (*n* = 4) relative to tubulin measured using Western blot. Measurements were performed on samples obtained from summer euthermic (SE), torpor late (TL), and arousal late (AL). Data represented as mean ± s.e.m. and are relative to the mean of SE. Statistical analysis by Kruskal-Wallis with Dunn's correction **P* < 0.05; ***P* < 0.01, *****P* < 0.0001

Note that although changes in differential expression are relatively limited (roughly FC = 2), these correspond closely to the order of magnitude of measured histone modification (by LC-MS/MS) and HDAC activity measurements. Lastly, considering DNA methylation, we observed overall DNA methylation remained unchanged between phases of hibernation as measured by LUMA and WGBS. This was in line with limited changes in the expression of known DNA methylation writers and erasers. Altogether, our study supports a role for histone acetylation changes associated with hibernation, which could be underlying the suppression of transcription in torpor.

Upregulation of SIRT2 and SIRT7 in arousal correlates to H4K16ac, linking epigenetics to hibernation

To identify whether deacetylation of histone in torpor was associated with particular erasers, we assessed their

RNA expression levels. Both *SIRT2* and *SIRT7* were upregulated during arousal. Partly corresponding with this observation, the liver tissue of ground squirrels displayed higher expression of SIRT1 and SIRT2 during torpor and of higher expression of SIRT3 during arousal [31, 32]. SIRT2 and SIRT7 both target H4K16ac as well as several other proteins [33]. Although SIRT2 and SIRT7 enzymes are predominantly located in the cytosol, they are able to translocate to the nucleus during G2/M transition (SIRT2) and/or in response to stress (SIRT7) where they can target H4K16ac [34]. Since it is known that the cell cycle is altered during hibernation (both torpor and arousal) and arousal is a stress-inducing event [35, 36], the upregulation of SIRT2 and SIRT7 could be responsible for lower acetylation levels of H4K16 during arousal in this study [33, 37]. As H4K16ac possesses the unique ability to both promote and inhibit the transcription of genes, it is particularly suitable to accommodate the dynamic nature of hibernation [38, 39]. Performing experiments on nuclear lysates could provide further support for the currently presented hypothesis. Lastly, SIRT2 and SIRT7 are known to be involved in glucose metabolism [40, 41], and hence potential candidates in facilitating the metabolic shift accompanying hibernation.

HDAC11 which we found to be lower expressed in arousal, mainly acts as a negative regulator of anti-inflammatory cytokine IL-10, and effects on histone acetylation levels have yet to be firmly demonstrated [42]. The downregulation of HDAC11 during arousal may play a role in the well-known suppression of inflammatory responses during hibernation phases [42–44].

Differential KAT6A, KAT6B, KAT7, and KAT13D expression is specific for the facultative hibernator, Syrian hamster

Previously, it has been shown in the liver tissue of hibernating squirrels that HAT protein expression, more specifically PCAF, is increased during torpor/arousal and expression of GCN5L2 is reduced compared to summer euthermic [15]. We found, contrasting to squirrel, that RNA expression of *PCAF* as well as *GCN5L2* were unchanged in Syrian hamster, suggesting that regulation of HAT during torpor in Syrian hamster differs from ground squirrel. Moreover, we report a lower level of H3K9ac during torpor, whereas other studies in hibernators show no differences in H3K9ac in the liver [15].

In ground squirrel, HAT activity was found to be stable throughout the torpor-arousal cycle [15], which could be confirmed in the Syrian hamster. Nonetheless, despite similar HAT activity, we found different expression levels of HAT encoding genes. The expression of *KAT6A* and *KAT13D* was significantly reduced during torpor, with overexpression of *KAT6A/KAT6B* and *KAT7* during arousal. Interestingly, it was recently described that the brain, but not the liver, retains circadian rhythm throughout hibernation [45]. As *KAT13D*, also known as CLOCK, is a known core circadian clock component [46], it is possible that *KAT13D* downregulation fuels delayed or paused circadian rhythm in the liver. Note that as European hamsters, obligatory hibernators from the same family as the Syrian hamster, do not show downregulation of CLOCK in the liver [47], this could also be a mechanism specific to facultative hibernators or Syrian hamster.

The present study confirms that in Syrian hamster liver, H3 acetylation, but not H3 protein levels, is affected during torpor, including decreased H3K18 and H3K23 acetylation in torpor and increased H3K27ac in arousal, similar to ground squirrel [17, 31, 48]. This observation may indicate a potential increase in chromatin condensation and a state of transcriptional repression in the liver during hibernation [49], whereas an increase in H3K27ac could result in open chromatin leading to transcriptional activation in arousing hamsters. The upregulation of *KAT6A* and *KAT6B* in arousal may therefore be associated with an increase in transcription through increased H3K27ac in arousal. Formation of such HAT complexes is indeed known to trigger aberrant histone acetylation and rapid transcriptional activation [50]. Both *KAT6A* and *KAT6B* have been shown to associate with multiple genes including CBP (CREB-binding protein) [50]. Of note, *KAT6A* and *KAT6B* proteins, through the formation of the MOZ/MORF complex, are responsible for acetylation of a number of protein lysines [50, 51]. Interestingly, among the top enriched transcription factor binding sites in promoter regions of genes upregulated during arousal in our hamsters was a suggested target for the MOZ/MORF complex, CREB1 [8]. Further research is warranted to confirm an increased transcriptional state in arousing hamsters through the formation of the MOZ/MORF complex.

HDAC6 activity is suggested to regulate protective pathways in torpor

Interestingly, using HDAC inhibitors, we found HDAC6 to constitute 71% of HDAC activity in the liver from all phases. As HDAC6 is an enzyme that can shuttle between the nucleus and the cytosol, it is often found to either regulate cytosolic tubulin and HSP90 acetylation, or nuclear histone acetylation [30]. The decreased H3ac levels (nuclear) and the increased acetylated α-tubulin (cytosolic) might suggest that HDAC6 resides in the nucleus during torpor, subsequently deacetylating H3 lysines. In addition to targeting histone lysines, HDAC6 is important for hepatic glucocorticoid receptor nuclear translocation of gluconeogenic genes [52]. Previously we have shown gluconeogenesis during torpor of these

hamsters through GO analysis using the RNA-seq data [8]. Although these results do not prove the necessity of HDAC6 in torpor regulation, we here suggest a role for HDAC6 in deacetylating H3- and H4Ks, thereby regulating RNA transcription and glucose metabolism during torpor. Inhibition of HDAC6 has been shown to result in hepatocellular protection in ischemia-induced liver injury [53], which suggests a role for HDAC6 for hepatocellular protection in Syrian hamster during hibernation. The mechanism underlying this protection is unknown, but HDAC6 has been shown to reduce oxidative stress and increase an anti-inflammatory response in cardiac ischemia [53, 54]. Furthermore, despite HDAC6 showing no differential expression between hibernation phases, it is known to interact with HDAC11 in humans [55] which is differentially expressed between hibernation phases. Collectively, the strong regulation of HDAC6 in torpor and its many links with torpor molecular pathways warrants further research into the subcellular location of HDAC6 and primary targets throughout hibernation to define its (epigenetic) role in cytoprotection.

Histone methylation and DNA methylation

Regarding histone methylation, our RNA-seq data showed that *KDM3A* expression is increased in arousal, *MLLT11* is downregulated in torpor, and *SETMAR* is downregulated in arousal. Despite the fact that only three histone (de)methylases are differentially expressed in hibernation, further research is required to investigate whether the differential expression of *KDM3A*, *MLLT11*, and *SETMAR* correlate to different histone methylation patterns, as was found in ground squirrel hibernation (H3K4me, H3K9me3) [56].

For DNA methylation, despite evidence for DNA methylation changes and changes in expression for DNA methylation writers and erasers during torpor in the greater horseshoe bat, *Rhinolophus ferrumequinum* [57] and other hibernators (see introduction), these findings could not be reproduced in Syrian Hamster and will thus likely not be major contributors in regulating hibernation phase switches. Nonetheless, more specific changes in DNA methylation, possibly modulating transcription factor activity, have been described in Syrian hamster [8].

Conclusion

We here present the first elaborate assessment of epigenetic marks (both histone modifications and DNA methylation) with combined assessment of expression levels of their respective writer and eraser proteins in a facultative hibernator, Syrian hamster. Our data show dynamic H3 and H4 acetylation during hibernation in the hamster liver. The increased activity of HDAC6 might be responsible for the previously reported transcriptional depression in torpor [58], although further study is necessary to confirm this hypothesis. Furthermore, differential acetylation of histone lysines during torpor (H3K18 and H3K23) and arousal (H3K23, H3K27, H4K12, and H4K16) were associated with the expression of several genes encoding histone-modifying enzymes genes. More specifically, SIRT2 and SIRT7 could modulate glucose metabolism in torpor and arousal, whereas HDAC11 likely is involved in immune response regulation. Additionally, *KAT6A*, *KAT6B*, *KAT7*, and *KAT13D* display significantly differential expression in accordance with observed changes in histone acetylation, previously not reported for obligatory hibernators and thus most likely specific for facultative hibernators or Syrian hamsters. Lastly, the expression of enzymes regulating DNA methylation and overall DNA methylation itself remained unchanged. In summary, our research suggests a role for histone acetylation (by modulation of acetylation writer and eraser expression) in the regulation of hibernation with its specificities for facultative hibernators.

Abbreviations

AE	Arousal early
AL	Arousal late
BAT	Brown adipose tissue
DNMT	DNA methyltransferase
HAT	Histone acetyltransferase
HDAC	Histone deacetylase
KDM	Histone demethylase
KMT	Histone methyltransferase
LUMA	Luminometric Methylation Assay
SE	Summer euthermic
SIRT	Sirtuin
TET	Ten-eleven translocation methylcytosine dioxygenase
TL	Torpor late
WB	Western blot
WGBS	Whole genome bisulfite sequencing

Supplementary Information

The online version contains supplementary material available at https://doi.org/10.1186/s43682-023-00024-2.

Additional file 1: Figure S1. Representative snapshot of western blot images. This figure contains a representative snapshot of WB images on which values in Figure 2 were based.

Additional file 2: Figure S2. HDAC activity measurement at various temperatures based on animal body temperature during different phases of hibernation. HDAC activity was measured at 8 °C, 22 °C and 37 °C corresponding with respectively animal body temperatures in Torpor Late (TL), Arousal Early (AE) and Summer Euthermic (SE). Respective differences between HDAC activity in different hibernation phases were retained, regardless of temperature at which HDAC activity measurements were obtained. dStatistical analysis was performed by Kruskal-Wallis with Dunn's correction $*P < 0.05$; $**P < 0.01$, $***P < 0.001$.

Additional file 3: Figure S3. HDAC activity with various inhibitors in liver of Syrian hamsters. HDAC activity in hamster liver ($n = 3$) using inhibitors: Entinostat to inhibit class I HDACs, Tubastatin A to inhibit HDAC6 and Vorinostat to inhibit all HDACs, except Sirtuins. Measurements were performed at samples obtained from Summer Euthermic (SE), Torpor Late

(TL), and Arousal Late (AL). Data represented as mean ± s.e.m. and are relative to the mean.

Additional file 4: Figure S4. DNA methylation in Syrian hamster liver measured by LUMA. Methylation measured using LUMA ($n = 4$). Measurements were performed at samples obtained from Summer Euthermic (SE), Torpor Late (TL), Arousal Early (AE) and Arousal Late (AL). Data represented as mean ± s.e.m. and are relative to the mean of SE. Statistical analysis by Kruskal-Wallis with Dunn's correction $*P < 0.05$.

Additional file 5: Figure S5. DNA methylation in Syrian hamster liver measured by WGBS. Boxplots for (A) CpG cytosine methylation, (B) non-CpG cytosine methylation, (C) promoter specific CpG cytosine methylation and (D) genic CpG cytosine methylation. Measurements were performed at samples obtained from Summer Euthermic (SE), Torpor Late (TL), Arousal Early (AE).

Additional file 6: Table S1. Table of animals characteristics. Characteristics for different animals used in this study.

Additional file 7: Table S2. Table of differentially expressed genes. Full results of differentially expressed genes for comparisons between SE vs TL, TL vs AE, SE vs AE and SE vs TL & AE)

Acknowledgements
Not applicable.

Authors' contributions
The first two authors contributed equally to this study. M.M.O obtained mRNA, gDNA and protein, performed HDAC assay and Western blots and wrote the manuscript. L.C. performed WGBS and analysis and wrote the manuscript. A.v.P and M.K performed chemical acetylation, in-solution digestion and LC-MS/MS including histone quantification. M.R.H.Z. performed HAT activity assay. V.A.R. and H.R.B wrote application and performed animal experiments. V.G. performed RNA sequencing. F.D., T.D.M, R.B., R.H.H and M.G.R supervised analyses and writing of the manuscript.

Funding
This study was financially supported by a Talent PhD scholarship to MMO by the Graduate School of Medical Sciences, University of Groningen, University Medical Center Groningen, and two grants from the Cock-Hadders Foundation, no. 2018-30 and 2019-52.

Availability of data and materials
The raw data for RNA sequencing and WGBS sequencing can be found in the Gene Expression Omnibus (GEO) under accessions GSE199814 and GSE199815. The mass spectrometry data have been deposited to the ProteomeXchange Consortium via the PRIDE partner repository with the dataset identifier PXD047797.

Declarations

Ethics approval and consent to participate
Experiments were approved by the Institutional Animal Ethical Committee of the University Medical Center Groningen. Animal procedures were carried out in accordance with the European Directive on the Protection of Animals used for Scientific Purposes and Dutch legislation.

Consent for publication
Not applicable.

Competing interests
The authors declare no competing interests.

Received: 15 December 2023 Accepted: 21 December 2023
Published online: 09 January 2024

References

1. Carey HV, Andrews MT, Martin SL. Mammalian hibernation: cellular and molecular responses to depressed metabolism and low temperature. Physiol Rev. 2003;83:1153–81.
2. Tessier SN, Storey KB. To be or not to be: the regulation of mRNA fate as a survival strategy during mammalian hibernation. Cell Stress Chaperon. 2014:763–76.
3. Al-attar R, Storey KB. Suspended in time: molecular responses to hibernation also promote longevity. Exp Gerontol. 2020;134(February):110889. https://doi.org/10.1016/j.exger.2020.110889.
4. Körtner G, Geiser F. The temporal organization of daily torpor and hibernation: circadian and circannual rhythms. Chonobiology Int. 2009;17(2):103–28.
5. Schwartz C, Andrews MT. Circannual transitions in gene expression: lessons from seasonal adaptations. Curr Top Dev Biol. 2013;105:247–73.
6. Janský L, Haddad G, Kahlerová Z, Nedoma J. Effect of external factors on hibernation of golden hamsters. J Comp Physiol-B Biochem Syst Environ Physiol. 1984;154(4):427–33.
7. Wijenayake S, Tessier SN, Storey KB. Metabolic arrest during hibernation! Cardiac regulation of pyruvate dehydrogenase (PDH) in a hibernating ground squirrel (Ictidomys tridecemlineatus). Can J Cardiol. 2015;31(10):S225. https://doi.org/10.1016/j.cjca.2015.07.475.
8. Coussement L, Oosterhof MM, Guryev V, Reitsema VA, Bruintjes JJ, Goris M, et al. Liver transcriptomic and methylomic analyses identify transcriptional mitogen- activated protein kinase regulation in facultative hibernation of Syrian hamster. Proc R Soc B Biol Sci. 2023:290.
9. Wang LHC. Advances in comparative and environmental physiology: animal adaptation to cold. Springer Science & Business Media; 2012.
10. Hannon JP, Vaughan DA. Initial stages of intermediary glucose catabolism in the hibernator and nonhibernator. Am J Physiol-Leg Content. 1961;201(2):217–23.
11. Serkova NJ, Rose JC, Epperson LE, Carey HV, Martin SL, Nj S, et al. Quantitative analysis of liver metabolites in three stages of the circannual hibernation cycle in 13-lined ground squirrels by NMR. Physiol Genomics. 2007;31:15–24.
12. Williams CT, Goropashnaya AV, Buck CL, Fedorov VB, Kohl F, Lee TN, et al. Hibernating above the permafrost: effects of ambient temperature and season on expression of metabolic genes in liver and brown adipose tissue of arctic ground squirrels. J Exp Biol. 2011;1300–6
13. Egervari BG, Glastad KM, Berger SL. Food for thought. Science. 2020;370(6517):695–711.
14. Biggar Y, Storey KB. Cryobiology Global DNA modifications suppress transcription in brown adipose tissue during hibernation q. Cryobiol. 2014;69(2):333–8. https://doi.org/10.1016/j.cryobiol.2014.08.008.
15. Rouble AN, Hawkins LJ, Storey KB. Roles for lysine acetyltransferases during mammalian hibernation. J Therm Biol. 2018;74(March):71–6. https://doi.org/10.1016/j.jtherbio.2018.03.013.
16. Morin PJ, Storey KB. Mammalian hibernation: differential gene expression and novel application of epigenetic controls. Int J Dev Biol. 2009;442(April):433–42.
17. Tessier SN, Luu BE, Smith JC, Storey KB. Cryobiology The role of global histone post-translational modifications during mammalian hibernation. Cryobiol. 2017;75:28–36. https://doi.org/10.1016/j.cryobiol.2017.02.008.
18. Tsukamoto D, Ito M, Takamatsu N. HNF-4 participates in the transcriptional regulation of the chipmunk hibernation-related protein gene. Nat Publ Gr. 2017:1–12.
19. Tsukamoto D, Ito M, Takamatsu N, Biochemical and Biophysical Research Communications. Epigenetic regulation of hibernation-associated HP-20 and HP-27 gene transcription in chipmunk liver. Biochem Biophys Res Commun. 2018;495(2):1758–65. https://doi.org/10.1016/j.bbrc.2017.12.052.
20. Gillen AE, Fu R, Riemondy KA, Jager J, Fang B, Lazar MA, et al. Liver transcriptome dynamics during hibernation are shaped by a shifting balance between transcription and RNA stability. Front Physiol. 2021;12:1–19.
21. Tessier SN, Ingelson-Filpula WA, Storey KB. Epigenetic regulation by DNA methyltransferases during torpor in the thirteen-lined ground squirrel Ictidomys tridecemlineatus. Mol Cell Biochem. 2021;476(11):3975–85. https://doi.org/10.1007/s11010-021-04214-1.
22. Alvarado S, Mak T, Liu S, Storey KB, Szyf M. Dynamic changes in global and gene-specific DNA methylation during hibernation in adult

thirteen-lined ground squirrels Ictidomys tridecemlineatus. J Exp Biol. 2015;218(11):1787–95.
23. Lin JQ, Huang YY, Bian MY, Wan QH, Fang SG. A unique energy-saving strategy during hibernation revealed by multi-omics analysis in the Chinese alligator. iScience. 2020;23(6):101202. https://doi.org/10.1016/j.isci.2020.101202.
24. Pinho GM, Martin JGA, Farrell C, Haghani A, Zoller JA, Zhang J, et al. Hibernation slows epigenetic ageing in yellow-bellied marmots. Nat Ecol Evol. 2022;6(4):418–26.
25. De Vrij EL, Vogelaar PC, Goris M, Houwertjes MC, Herwig A, Dugbartey GJ, et al. Platelet dynamics during natural and pharmacologically induced torpor and forced hypothermia. PLoS One. 2014;9(4):1–12.
26. Oklejewicz M, Daan S, Strijkstra AM. Temporal organisation of hibernation in wild-type and tau mutant Syrian hamsters. J Comp Physiol - B Biochem Syst Environ Physiol. 2001;171(5):431–9.
27. van Pijkeren A, Dietze J, Brotons AS, Egger AS, Lijster T, Barcaru A, et al. Combined metabolic and chemical (CoMetChem) labeling using stable isotopes—a strategy to reveal site-specific histone acetylation and deacetylation rates by LC-MS. Anal Chem. 2021;93(38):12872–80.
28. Butler KV, Kalin J, Brochier C, Vistoli G, Langley B, Kozikowski AP, et al. Rational design and simple chemistry yield a superior, neuroprotective HDAC6 inhibitor, tubastatin A. J Am Chem Soc. 2010;(4):10842–6.
29. Leus NGJ, Van Den BT, Van Der WPE, Krist K, Ourailidou ME, Eleftheriadis N, et al. HDAC1-3 inhibitor MS-275 enhances IL10 expression in reduces cigarette smoke-induced airway inflammation in mice. Nat Publ Gr. 2017:1–18.
30. Zhang Y, Li N, Caron C, Matthias G, Hess D, Khochbin S, et al. HDAC-6 interacts with and deacetylates tubulin and microtubules in vivo. EMBO J. 2003;22(5):1168–79.
31. Morin PJ, Storey KB. Evidence for a reduced transcriptional state during hibernation in ground squirrels. Cryobiol. 2006;53:310–8.
32. Rouble AN, Storey KB. Cryobiology Characterization of the SIRT family of NAD + -dependent protein deacetylases in the context of a mammalian model of hibernation , the thirteen-lined ground squirrel. Cryobiol. 2015;71(2):334–43. https://doi.org/10.1016/j.cryobiol.2015.08.009.
33. Tang BL. SIRT7 and hepatic lipid metabolism. Front Cell Develop Biol. 2015;3(January):1–3.
34. Chen S, Seiler J, Santiago-reichelt M, Felbel K, Grummt I, Voit R. Repression of RNA polymerase I upon stress is caused by inhibition of RNA-dependent deacetylation of PAF53 by SIRT7. Mol Cell. 2013;52(3):303–13. https://doi.org/10.1016/j.molcel.2013.10.010.
35. Carey HV, Sills NS, Gorham DA. Stress proteins in mammalian hibernation. Am Zool. 1999;39(6):825–35.
36. Wu CW, Storey KB. Pattern of cellular quiescence over the hibernation cycle in liver of thirteen-lined ground squirrels. Cell Cycle. 2012;11(9):1714–26.
37. Jiang W, Wang S, Xiao M, Lin Y, Zhou L, Lei Q, et al. Article acetylation regulates gluconeogenesis by promoting PEPCK1 degradation via recruiting the UBR5 ubiquitin ligase. Mol Cell. 2011;43(1):33–44. https://doi.org/10.1016/j.molcel.2011.04.028.
38. Blosser TR, Yang JG, Stone MD, Narlikar GJ, Zhuang X. Dynamics of nucleosome remodelling by individual ACF complexes. Nature. 2009:462.
39. Taylor GCA, Eskeland R, Pradeepa MM, Bickmore WA. H4K16 acetylation marks active genes and enhancers of embryonic stem cells, but does not alter chromatin compaction. Genome Res. 2013;23:2053–65.
40. Watanabe H, Inaba Y, Kimura K, Matsumoto M, Kaneko S, Kasuga M, et al. Sirt2 facilitates hepatic glucose uptake by deacetylating glucokinase regulatory protein. Nat Commun. 2018;9(1):1–14. https://doi.org/10.1038/s41467-017-02537-6.
41. Mizumoto T, Yoshizawa T, Sato Y, Ito T, Tsuyama T, Satoh A, et al. SIRT7 deficiency protects against aging-associated glucose intolerance and extends lifespan in male mice. Cells. 2022;11(22):1–15.
42. Cao J, Sun L, Aramsangtienchai P, Spiegelman NA, Zhang X, Huang W. HDAC11 regulates type I interferon signaling through. Proc Natl Acad Sci U S A. 2019;116(12):5487–92.
43. Andrews MT. Molecular interactions underpinning the phenotype of hibernation in mammals. J Exp Biol. 2019;222(2)
44. Reitsema VA, Oosterhof MM, Henning RH, Bouma HR. Phase specific suppression of neutrophil function in hibernating Syrian hamster. Dev Comp Immunol. 2021;119:5.
45. Borah BK, Renthlei Z, Trivedi AK. Hypothalamus but not liver retains daily expression of clock genes during hibernation in terai tree frog (Polypedates teraiensis). Chronobiol Int. 2020;37(4):1058–67.
46. Ko CH, Takahashi JS. Molecular components of the mammalian circadian clock. Hum Mol Genet. 2006;15(SUPPL. 2):271–7.
47. Gautier C, Bothorel B, Ciocca D, Valour D, Gaudeau A, Dupré C, et al. Gene expression profiling during hibernation in the European hamster. Sci Rep. 2018;8(1):1–17.
48. Wijenayake S, Storey KB. Dynamic regulation of histone H3 lysine (K) acetylation and deacetylation during prolonged oxygen deprivation in a champion anaerobe. Mol Cell Biochem. 2020;474(1):229–41. https://doi.org/10.1007/s11010-020-03848-x.
49. Lin R, Wu J, You Z, Xu D, Li C, Wang W, et al. Induction of hibernation and changes in physiological and metabolic indices in Pelodiscus sinensis. Biology (Basel). 2023;12(5):1–16.
50. Klein BJ, Lalonde M-E, Côté J, Yang X-J, Kutateladze TG. Crosstalk between epigenetic readers regulates the MOZ/MORF HAT complexes. Epigenetics. 2014;9(2):186–93.
51. Carlson S, Glass KC, Sciences H. The MOZ histone acetyltransferase in epigenetic signaling and disease. J Cell Physiol. 2014;229(11):1571–4.
52. Winkler R, Benz V, Clemenz M, Bloch M, Foryst-ludwig A, Wardat S, et al. Histone deacetylase 6 (HDAC6) is an essential modifier of glucocorticoid-induced hepatic gluconeogenesis. Diabetes. 2012;61(February):513–23.
53. Concors S, Murken D, Aufhauser DD, Wang Z, Ge G, Hancock WW, et al. Histone deacetylase-6 inhibition is protective in liver ischemia-reperfusion injury and acetaminophen toxicity in a murine model. Transplantation. 2018;102. https://doi.org/10.1097/01.tp.0000543094.36277.44.
54. Pickell Z, Williams AM, Alam HB, Hsu CH. Histone deacetylase inhibitors: a novel cardioprotection following ischemia. J Am Heart Assoc. 2020:1–11.
55. Gao L, Cueto MA, Asselbergs F, Atadja P. Cloning and functional characterization of HDAC11, a novel member of the human histone deacetylase family. J Biol Chem. 2002;277(28):25748–55. https://doi.org/10.1074/jbc.M111871200.
56. Watts AJ, Storey KB. Hibernation impacts lysine methylation dynamics in the 13-lined ground squirrel Ictidomys tridecemlineatus. J Exp Zool. 2019;331:234–44.
57. Liu S, Wang X, Zhu Y, Guo D, Wang Y, Wang Y. Epigenetic changes between the active and torpid states in the greater horseshoe bat (Rhinolophus ferrumequinum). Comp Biochem Physiol Part - B Biochem Mol Biol. 2022;2023(265):1–5.
58. Van Breukelen F, Martin SL. Reversible depression of transcription during hibernation. J Comp Physiol B Biochem Syst Environ Physiol. 2002;172(5):355–61.

Publisher's Note